CONF-960643--2

Janet Pawel Robertson[1], Ikuo Ioka[2], Arthur F. Rowcliffe[3], Martin L. Grossbeck[1], and Shiro Jitsukawa[4]

TEMPERATURE DEPENDENCE OF THE DEFORMATION BEHAVIOR OF TYPE 316 STAINLESS STEEL AFTER LOW TEMPERATURE NEUTRON IRRADIATION

REFERENCE: Robertson, J. P., Ioka, I., Rowcliffe, A. F., Grossbeck, M. L., and Jitsukawa, S., "Temperature Dependence of the Deformation Behavior of Type 316 Stainless Steel after Low Temperature Neutron Irradiation," Effects of Radiation on Materials: 18th International Symposium, ASTM STP 1325, R. K. Nanstad, M. L. Hamilton, F. A. Garner, and A. S. Kumar, Eds., American Society for Testing and Materials, Philadelphia, 1997.

ABSTRACT: The effects of low temperature neutron irradiation on the tensile behavior of type 316 stainless steel were investigated. A single heat of solution annealed type 316 stainless steel was irradiated to 7 and 18 dpa at 60, 200, 330, and 400°C. The tensile properties as a function of dose and as a function of temperature were examined. Large changes in yield strength, deformation mode, strain to necking, and strain hardening capacity were seen in this irradiation experiment. The magnitudes of the changes are dependent on both irradiation temperature and neutron dose. Irradiation can more than triple the yield strength over the unirradiated value and decrease the strain to necking (STN) to less than 0.5% under certain conditions. A maximum increase in yield strength and a minimum in the STN occur after irradiation at 330°C but the failure mode remains ductile.

KEYWORDS: austenitic stainless steel, tensile properties, neutron irradiation, spectrally tailored experiment

[1]Research staff, Metals and Ceramics Division, Oak Ridge National Laboratory, Oak Ridge, Tennessee, 37831-6376, USA
[2]Senior engineer, Department of Materials Science and Engineering, Japan Atomic Energy Research Institute, Tokai-mura, Ibaraki-ken 319-11, Japan
[3]Group leader, Metals and Ceramics Division, Oak Ridge National Laboratory, Oak Ridge, Tennessee, 37831-6376, USA
[4]Senior research engineer, Department of Materials Science and Engineering, Japan Atomic Energy Research Institute, Tokai-mura, Ibaraki-ken 319-11, Japan

DISCLAIMER

Austenitic stainless steels will be used in first wall/shield (FW/S) structures for near term fusion machines such as the International Thermonuclear Experimental Reactor (ITER). These steels have favorable strength, toughness, and fabrication properties, and there is an enormous reservoir of experience in fabricating and operating code qualified austenitic stainless steel components in nuclear systems. The proposed dose/temperature operating conditions for ITER are below the regimes for void swelling (400-600°C) and for grain boundary embrittlement (≥500°C); however, mechanical properties such as yield strength, ductility, and strain hardening capacity change rapidly with dose at these low temperatures [1-3]. These changes in mechanical properties are also dependent on irradiation temperature. In the vicinity of 300°C, neutron-irradiated austenitic steels undergo a transition in microstructure from a low temperature regime dominated by black dots to a high temperature regime dominated by Frank loops and small cavities [4,5]. This transition as a function of temperature is apparent in the tensile response of specimens irradiated in this low temperature regime.

A reactor irradiation experiment has been conducted in the Oak Ridge Research Reactor and the High Flux Isotope Reactor to quantify the effects of neutron irradiation on the tensile behavior of austenitic stainless steels irradiated to doses up to 18 dpa at temperatures from 60 to 400°C. In each reactor, the thermal to fast neutron flux ratio was tailored using thermal neutron shields such that the helium generation rate in type 316 stainless steel was within the range expected for a fusion first wall and shield, about 10-20 appm He/dpa. For this paper, the tensile data from a single heat of type 316 solution annealed material have been examined, and both the dose dependence and the temperature dependence of the changes in tensile properties are discussed. Some insights into the dose-temperature regime in which the tensile properties are most severely affected by neutron irradiation and the microstructural features of this regime are presented.

EXPERIMENTAL PROCEDURES

The composition of the solution annealed (SA) type 316 stainless steel material (designated J316) irradiated in this experiment is given in Table 1. The specimens were in the form of SS-1 flat tensile specimens with an overall length of 44.45 mm. The gage section of this type of specimen is 20.32 mm long, 1.52 mm wide, and 0.76 mm thick.

The irradiation experiment was conducted in two stages. In the first stage, the tensile specimens were irradiated in the Oak Ridge Research Reactor (ORR) at temperatures of 60, 200, 330, and 400°C to a peak damage level of about 7 dpa (9×10^{21} n/cm^2, E>0.1 MeV) [6-9]. The dual-temperature irradiation capsules used for this stage were designated ORR-MFE-6J (which operated at 60 and 200°C) and ORR-MFE-7J (which operated at 330 and 400°C). The 60°C capsule region was cooled directly with reactor cooling water. The 200°C temperature was maintained by conduction of heat through aluminum holders. The temperatures of the higher temperature regions, 330 and 400°C, were monitored and controlled during irradiation by modifying the composition of the thermal conduction gas surrounding the specimens. The details of this irradiation are described in Table 2 and elsewhere [6-8].

TABLE 1--Alloy composition of J316.

	Composition (wt %)									
Alloy	Fe	Ni	Cr	Ti	Mo	Mn	Si	C	P	S
J316	Bal	13.5	16.8	0.005	2.46	1.80	0.61	0.058	0.028	0.003

TABLE 2--Maximum neutron fluence values accumulated in each capsule.

	Experiment Designation					
Neutron Fluence, $\times 10^{21}$ n/cm^2	ORR -MFE -6J (60 and 200°C)	ORR -MFE -7J (330 and 400°C)	HFIR -MFE -60J-1 (60°C)	HFIR -MFE -200J-1* (200°C)	HFIR -MFE -330J-1 (330°C)	HFIR -MFE -400J-1* (400°C)
Total	24.0	27.0	39.5	33.3	39.5	33.3
Thermal (<0.5 eV)	6.71	8.07	4.71	3.97	4.71	3.97
0.5 eV- 0.1 MeV	8.55	9.46	15.4	13.0	15.4	13.0
>0.1 MeV	8.76	9.47	19.4	16.4	19.4	16.4
>1 MeV	4.84	5.14	7.04	5.93	7.04	5.93

*Estimated from reactor power data

Some of these specimens were then re-encapsulated into irradiation capsules designed to operate in the removable beryllium (RB) positions of the High Flux Isotope Reactor (HFIR). The capsules were designed such that the test specimens were irradiated at the same temperature as in the first stage of the irradiation. The capsules were designated HFIR-MFE-RB-60J-1, 200J-1, 330J-1 and 400J-1. A 4.2 mm thick hafnium shield surrounded the capsules in the HFIR in order to reduce the thermal neutron flux and maintain a He/dpa level near that expected in a fusion reactor for the combined two stage experiment. The 60J-1 and 330J-1 capsules accumulated a peak dose of approximately 12 dpa (1.9 $\times$ 10^{22} n/cm^2, E > 0.1 MeV) [10] in the HFIR (in addition to 7 dpa in the ORR). The 200J-1 and 400J-1 capsules accumulated a peak dose of approximately 10 dpa in the HFIR in addition to 7 dpa in the ORR (the analysis of the dosimetry for the 200J-1 and 400J-1 capsules is still in progress). Details of the irradiation can be found in Table 2 and elsewhere [10-12]. For the purposes of this report, the lower dose level will be referred to as 7 dpa and the higher dose level as 18 dpa.

The transmutation of Ni-58 to Ni-59 and then to Fe-55 and helium can be calculated from the dosimetry results. The irradiation in the ORR produced approximately 75-100 appm He in the steel, giving a He/dpa ratio of about 11 appm/dpa. Continued irradiation in the HFIR resulted in a total of approximately 188 appm He in 60J-1 and 225 appm He in 330J-1 [10]. The helium content calculation was confirmed by isotope-dilution gas mass spectrometry [10]. This HFIR irradiation, combined with the ORR irradiation, resulted in a helium to displacement ratio of 10.2 appm He/dpa in 60J-1 and 11.8 appm He/dpa in 330J-1. It is estimated that the combined 6J/200J-1 and the 7J/400J-1 experiments resulted in about 10-12 appm He/dpa. These data are summarized in Table 3.

TABLE 3--Maximum damage and accumulated helium for type 316 stainless steel.*

Experiment	dpa	appm He†
ORR-MFE-6J	6.9	75
ORR-MFE-7J	7.4	102
HFIR-MFE-60J-1	11.6	113
HFIR-MFE-200J-1	9.9‡	92‡
HFIR-MFE-330J-1	11.6	123
HFIR-MFE-400J-1	9.9‡	101‡
6J + 60J-1	18.5	188
6J + 200J-1	16.8‡	167‡
7J + 330J-1	19.0	225
7J + 400J-1	17.3‡	203‡

*type 316 stainless steel: Fe (0.645), Ni (0.13), Cr (0.18), Mn (0.019), Mo (0.026) wt%

†HFIR data assume the previous exposure in the ORR; this is important for the accurate calculation of the Ni-59 burn-in

‡Estimated from reactor power data

The operating temperature of the HFIR-MFE-RB-60J-1 capsule was 60°C, with the specimens in direct contact with the reactor cooling water. The HFIR-MFE-RB-200J-1, 330J-1, and 400J-1 capsules operated at 200, 330, and 400°C, respectively, with the temperature actively controlled as before by changing the gas mixture around the specimen holder in response to 21 thermocouples located inside the holder. Thermocouple data and detailed discussions of the capsule operations are given in the references [12,13].

Tensile testing was conducted on an Instron universal testing machine. The specimens irradiated at 60°C (from the 60J-1 capsule) were tested at room temperature (25°C) in air. The specimens irradiated at 200, 330, and 400°C (from 200J-1, 330J-1, and 400J-1, respectively) were tested at the irradiation temperature under vacuum. In each case, the strain rate was 0.0004/s. The 0.2% offset yield strength (YS), ultimate tensile strength (UTS), uniform elongation (E_u), and total elongation (E_t) were calculated from the engineering load-elongation curves. At least two specimens were tested for each experimental condition.

The appropriateness of the conventional methods of determining uniform strain in irradiated materials is a subject of current debate [14-16]. The standard approach to determining the extent of uniform elongation utilizes the point of maximum stress in the engineering stress-strain curve. For unirradiated material, the maximum engineering stress defines the point at which the strain hardening capacity is exhausted and the next local area contraction, which raises the true stress, is no longer balanced by an increase in strength. Additional plastic deformation is localized in the necked region. Irradiation and testing at temperatures below about 350°C result in an engineering stress-strain curve in which a load drop occurs just after yielding. As the test continues, the load increases again, sometimes only slightly, and the material continues to deform at a low work-hardening rate. Thus, the observed local maximum load that occurs just after yielding should not be used as the point for measurement of uniform elongation

[3,17]. Horsten and de Vries [16,18-20] have studied this situation by repeatedly loading and unloading a specimen and measuring the dimensions of the gage section. They were able to show that, following the initial load drop after yielding, deformation occurs uniformly up to the point where the engineering stress-strain curve undergoes a rapid downturn prior to fracture, the so-called strain to necking (STN) [16,18,19]. The STN was also measured from the engineering stress-strain curves.

RESULTS

The tensile data for the J316 solution annealed specimens are given in Table 4. Typical engineering stress-strain curves for the solution annealed material are shown in Figs. 1-4. Zero strain in these figures is set where the modulus line extrapolates to the x-axis; however, this is not a true modulus line since it includes machine load train deflection.

Irradiation at 60°C (Fig. 1) results in a greater than twofold increase in yield stress. The smooth yielding behavior of the unirradiated material is replaced by the appearance of a small yield drop. Following the yield drop, the irradiated material work hardens at a much lower rate than in the unirradiated condition but still elongates more than 20% before necking and failure occur. At both 7 and 18 dpa, the UTS is higher than the YS by less than 10%. While there is no significant yield strength increase from 7 to 18 dpa, the strain to necking and the total elongation are both reduced with this dose increment.

After irradiation and testing at 200°C (Fig. 2), the yield stress is almost three times higher than the unirradiated value. The material work hardens only slightly, with the maximum in the engineering stress-strain curve sometimes occurring at the upper yield point. The yield strength is the same (745 MPa) after irradiation to both 7 and 18 dpa. However, the STN and the total elongation continue to decrease with the dose increment from 7 to 18 dpa. The strain to necking is 8-14% after 7 dpa but drops to only 3-7% after 18 dpa. Total elongation remains high at 15 to 20% after 7 dpa but is only 6-10% after 18 dpa.

After irradiation and testing at 330°C (Fig. 3), the deformation behavior is significantly different. The yield strength increases from the unirradiated value of about 250 MPa to more than 850 MPa at 7 dpa, an increase of 250%. The increase in yield stress is greater than the increase seen at 60°C by about 150 MPa. The yield stress only increases about 5% from 7 to 18 dpa. After yielding, the characteristic yield drop is apparent, but the material does not exhibit any work hardening capability. The applied load falls rapidly and failure occurs after only about 3% total elongation. The strain to necking is less than 0.5% in each case. The failure mode, however, is ductile [3].

Irradiation and testing at 400°C show another regime as a function of temperature (Fig. 4), and result in the least amount of hardening (increase in yield strength) of the four temperature sets and more work hardening than at 200 or 330°C. There is no evidence of the yield drop seen after irradiation at lower temperatures. The yield strength increases from 237 MPa to 623 MPa at 7 dpa, and then increases an additional 4% at 18 dpa. The strain to necking is much greater than that at 330°C, but is still less than 6%.

TABLE 4--Tensile data from solution annealed J316 irradiated in the ORR and HFIR spectrally tailored experiment.

Specimen number	dose, dpa	irradiation temp., °C	test temp., °C	YS, MPa	UTS, MPa	STN, %	Eu, %	Et, %	He level, appm	appm He/dpa	Reactor
EL61	0	...	25	327	602	50.4	50.4	56.5	...	...	...
EL26	0	...	25	283	552	49.5	49.5	54.0	...	...	...
EL30	0	...	200	254	492	31.9	31.9	36.2	...	...	...
EL62	0	...	200	263	503	31.3	31.3	34.6	...	...	...
EL31	0	...	330	230	484	28.8	28.8	31.3	...	...	...
EL63	0	...	330	262	508	28.4	28.4	34.6	...	...	...
EL32	0	...	400	252	476	26.1	26.1	28.4	...	...	...
EL64	0	...	400	222	476	33.0	33.0	35.1	...	...	...
EL33	6.9	60	25	703	752	26.1	24.5	29.9	100	14.5	ORR
EL34	6.9	60	25	690	745	29.9	27.6	32.5	100	14.5	ORR
EL44	6.9	200	200	758	765	13.6	0.2	15.9	100	14.5	ORR
EL46	6.9	200	200	733	737	12.0	11.5	14.5	100	14.5	ORR
EL1	7.4	330	330	848	855	0.3	0.3	3.1	100	13.5	ORR
EL2	7.4	330	330	869	869	0.3	0.3	2.9	100	13.5	ORR
EL14	7.4	400	400	595	677	5.1	4.6	7.0	100	13.5	ORR
EL15	7.4	400	400	650	717	4.9	4.3	6.8	100	13.5	ORR
EL36	18.5	60	25	716	743	22.2	20.4	24.6	188	10.2	ORR+HFIR
EL37	18.5	60	25	747	765	23.3	20.4	25.6	188	10.2	ORR+HFIR
EL48	17.0	200	200	745	752	3.4	0.2	5.7	197	11.6	ORR+HFIR
EL49	17.0	200	200	740	740	7.2	0.2	9.8	197	11.6	ORR+HFIR
EL04	19.0	330	330	903	913	0.4	0.4	3.1	224	11.8	ORR+HFIR
EL05	19.0	330	330	909	921	0.4	0.4	3.1	224	11.8	ORR+HFIR
EL17	17.0	400	400	663	720	2.4	2.4	4.3	197	11.6	ORR+HFIR
EL20	17.0	400	400	634	716	5.8	5.8	8.1	197	11.6	ORR+HFIR

The 0.2% offset yield strengths as a function of neutron dose are plotted for each temperature in Fig. 5. For all four irradiation temperatures, irradiation to about 7 dpa resulted in a yield strength increase over the unirradiated value of 130-250%. Additional irradiation to 18 dpa caused further increases in the yield strength of less than 5%. Under these conditions for this alloy, the yield strength has essentially saturated with dose by 7 dpa. These data are consistent with data taken from the literature for a variety of austenitic stainless steels irradiated at low (less than 250°C) temperatures. Prior to irradiation, type 316 steels have room temperature yield strengths in the range of 225-350 MPa and the YS decreases slightly with increasing temperature. After even modest irradiation levels of about

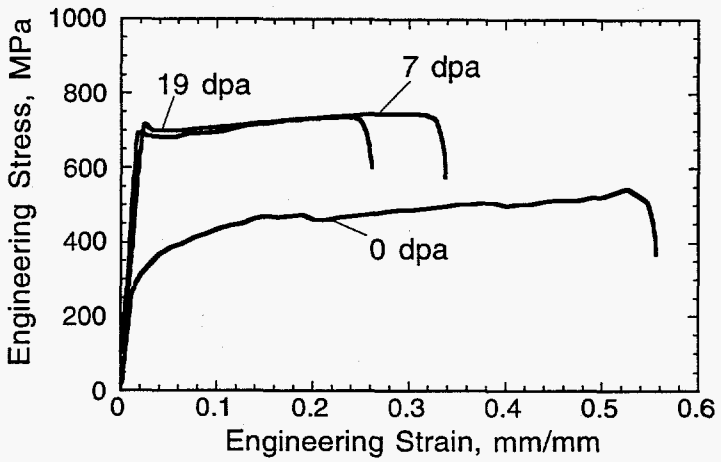

FIG. 1--Typical engineering stress-strain curves for SA J316 irradiated at 60°C and tested at 25°C.

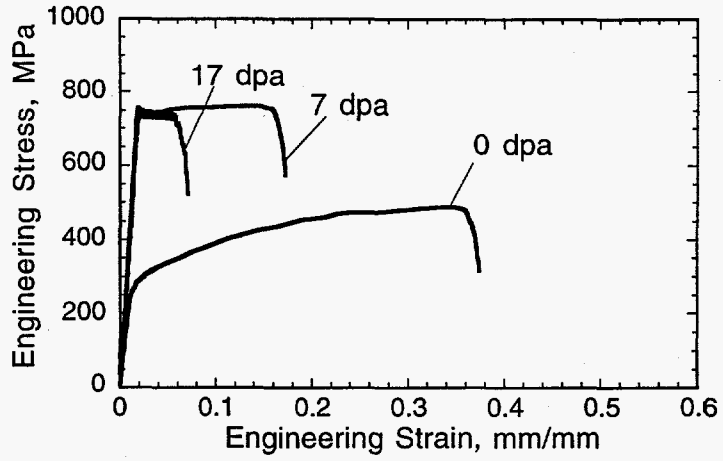

FIG. 2--Typical engineering stress-strain curves for SA J316 irradiated and tested at 200°C.

1 dpa at low temperatures, the yield strength increases by several hundred MPa. For example, Tavassoli [21] reported significant increases in yield and ultimate tensile strengths at displacement levels less than 1 dpa and saturation of these strengths at approximately 3 dpa for type 316LN stainless steel irradiated at temperatures less than 400°C. Kallstrom et al. [22] irradiated type 316LN stainless steel to only 0.3 dpa at 35°C and reported a yield strength of 552 MPa after testing at 75°C. Heinisch [23] also reported significant increases in the yield strength of type 316 as the result of very low dose irradiations (<0.01 dpa). These data are shown in Fig. 6 along with other data from the literature. The rate of yield strength increase slows with increasing neutron dose and a saturation value is approached in the range of 1 to 3 dpa. This observation is generally consistent with microstructural data, which indicate that the doses necessary to

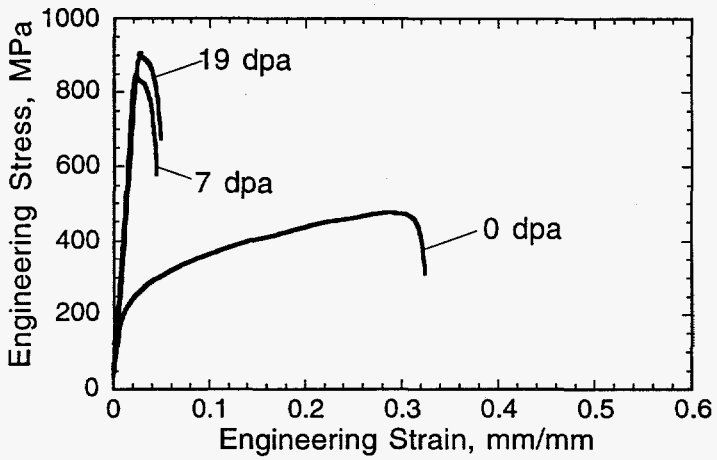

FIG. 3--Typical engineering stress-strain curves for SA J316 irradiated and tested at 330°C.

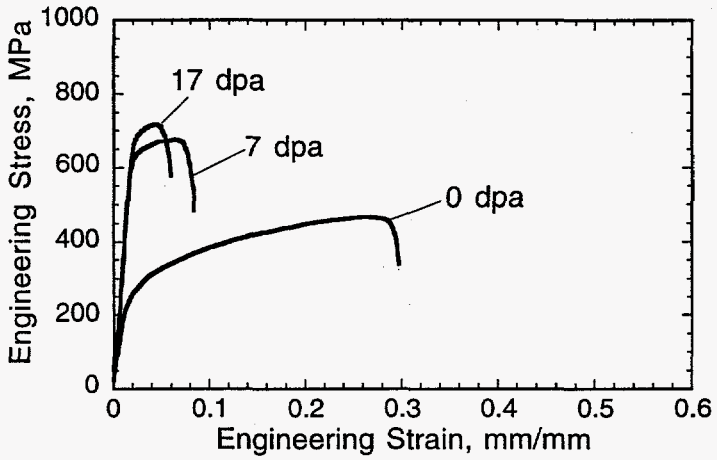

FIG. 4--Typical engineering stress-strain curves for SA J316 irradiated and tested at 400°C.

approach the saturation of the black dot and loop densities, although somewhat dependent on irradiation temperature, are about 0.1 and ≥1 dpa, respectively [4].

Before irradiation, the ultimate tensile strengths are 240-270 MPa (84-114%) higher than the corresponding yield strengths. The ultimate tensile strengths after irradiation at temperatures less than or equal to 330°C are only slightly higher (<8%) than the corresponding yield strengths and follow the same trends as yield strength with dose. Literature data also reveal that the YS approaches the UTS for irradiations ≤ 350°C or so [14,24,33-35], indicative of the loss of strain hardening capacity. After irradiation at 400°C, the UTS values are 8-14% higher than the yield strengths.

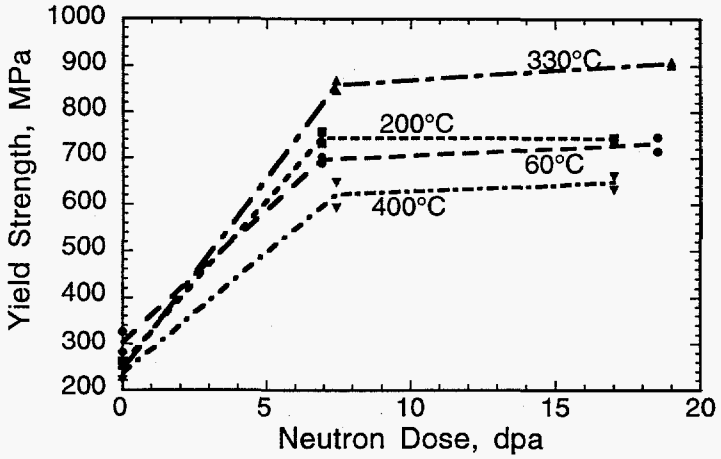

FIG. 5--Yield strength as a function of neutron dose. The irradiation and test temperature are shown in the figure.

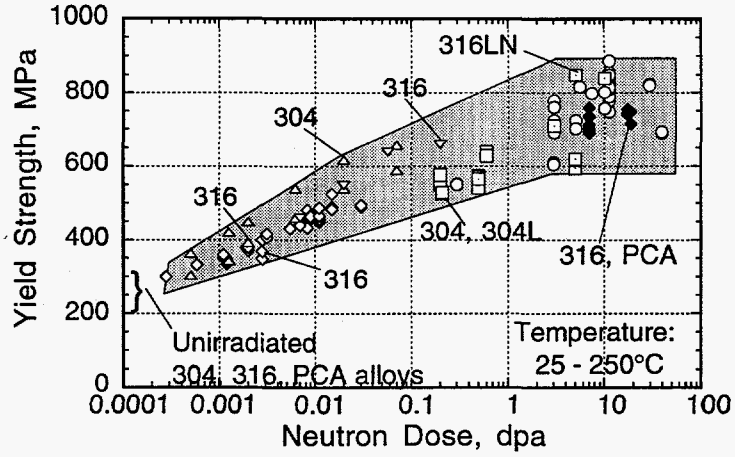

FIG. 6--Yield strength as a function of neutron dose for type 304, 316, and titanium-modified (PCA) austenitic stainless steels irradiated in a variety of experiments. In each case, the test temperature equals the irradiation temperature and is in the range of 25-250°C [1,2,15,16,18, 19,21-32].

The strain to necking values are shown as a function of dpa and temperature in Fig. 7. At 25°C, the unirradiated values are very high, about 50%. At the higher test temperatures, the unirradiated values are about 30%. The STN drops off quickly with dose at each temperature, with the decline most severe for the 330°C case. After irradiation to both 7 and 18 dpa at 60°C, the STN remains high, greater than 25%. Irradiation at 200°C results in STN of more than 12% at 7 dpa, but only 3-7% after 18 dpa. Irradiation at 330°C results in STN less than 1% at each dose, with total elongations of only 3%. Elongations increase slightly at 400°C over those at 330°C. The STN continues to drop with increasing dose from 7 to 18 dpa for the 60°C irradiation and even the

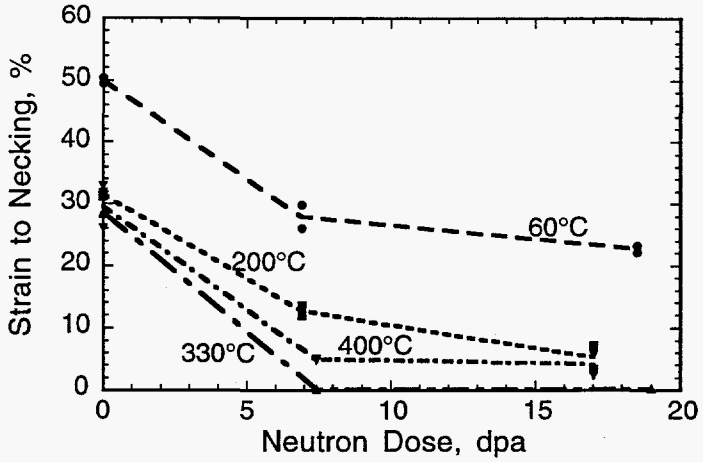

FIG. 7--Strain to necking as a function of neutron dose. The irradiation and test temperature are shown in the figure.

200°C irradiation, which showed no increase in the hardening after 7 dpa. The STN change has essentially saturated with dose by 7 dpa for the 330 and 400°C irradiations. In general, for irradiation and test temperatures up to about 250°C, the strain to necking values are high, even after irradiation to about 10 dpa. In the 250-350°C regime, however, the strain to necking values appear to fall off quickly after irradiation to doses higher than 3 dpa [1,2,15,16,18,19,22,24-28,30,36].

One of the unique features of this experiment was the irradiation of the same heat of J316 in capsules under the same reactor conditions with precise temperature control. The changes in tensile properties as a function of temperature may influence the ITER desired operating regime and it is useful to reiterate the data in the form of property versus temperature plots in which the trends with irradiation temperature are more clearly seen. Figure 8 shows typical engineering stress-strain curves for the J316 solution annealed material irradiated in the ORR to 7 dpa at each temperature. The high yield stress, the loss of work hardening, and the rapid failure after 330°C irradiation are particularly evident.

The solution annealed J316 material irradiated to 7 dpa showed a peak in the yield strength as a function of temperature at 330°C (Fig. 9). The 18 dpa data superimposed on this figure for comparison follow the same trend. Composite plots of yield strength as a function of irradiation temperature for solution annealed austenitic stainless steel variants have been generated from literature data [e.g., 37]. For specimens irradiated up to 20 dpa in a variety of reactors, these combined data also reveal a maximum in yield strength around 300°C in spite of the many different experimental variables.

Three regimes of STN have been designated based on the discussion by Majumdar [38] on design rules for ITER components. For E_u values greater than 5%, the material is considered to be sufficiently ductile for ASME Code rules to be applicable. For the semi-brittle (1% < E_u <5%) and brittle (E_u <1%) regimes, a different set of design rules to

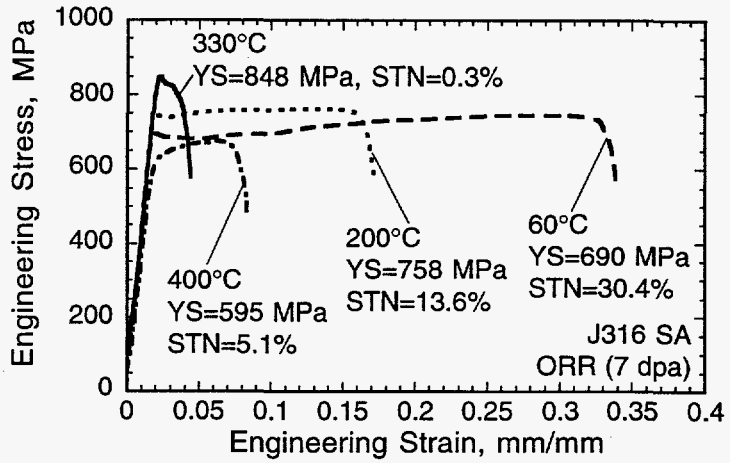

FIG. 8--Typical engineering stress-strain curves for SA J316 irradiated to 7 dpa at 60, 200, 330, and 400°C. The 0.2% offset YS and the STN are given in the figure for each curve.

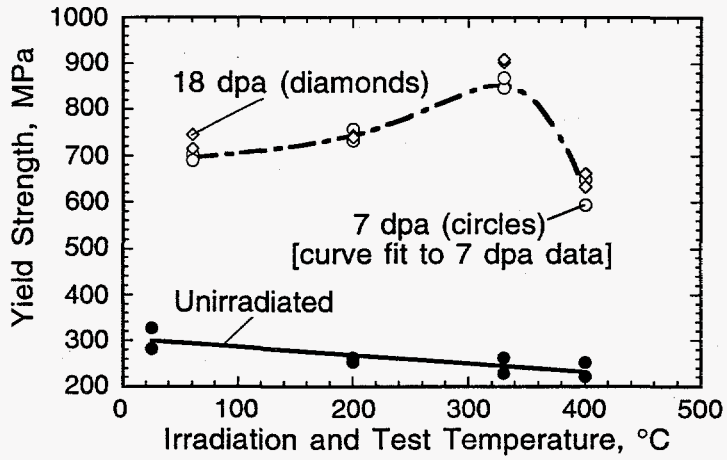

FIG. 9--Yield strength as function of temperature (the irradiation temperature equals the test temperature) for both the 7 and 18 dpa dose levels.

protect against failure by plastic collapse in regions of high stress concentration needs to be adopted. As previously discussed, STN is a more appropriate measure of ductility for irradiated materials than is uniform elongation. The STN values measured in the experiment reported here have been combined with other data from the literature [1,2,16,18, 22,24,25,27,39,40] in the form of a damage-temperature map (Fig. 10). STN values less than 1% are represented by closed circles in Fig. 10. In this regime, the yield stress is increased by more than a factor of three above the unirradiated value, the material has zero strain hardening capacity, and, following the initial load drop, strain is intensely localized (e.g., Fig. 3). Although a failure with less than 1% STN is frequently classified as "brittle" for design code purposes,

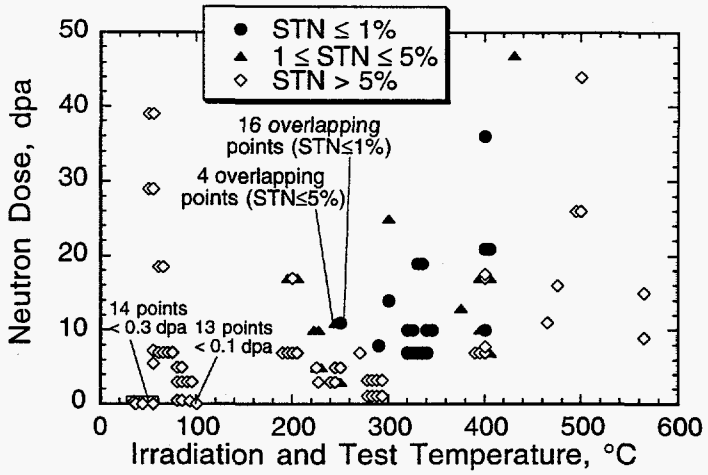

FIG. 10--Strain to necking as a function of neutron dose and temperature for solution annealed austenitic stainless steels [1,2,16,18,22,24,25,27,39,40]. Several sets of overlapping data are noted on the figure. Horizontal sets of data represent the same nominal irradiation temperature: the distribution is used to distinguish otherwise overlapping points.

failure actually occurs in a ductile tearing mode [3] as opposed to brittle cleavage. Significant post-necking ductility is still retained even in the regime where the material undergoes plastic instability immediately after yielding. For example, other experiments have shown that the reduction in area (RA), which is used to measure the true strain at failure, of type 316LN stainless steel decreases from an unirradiated value of about 70% to about 60% after irradiation to 11 dpa at 250°C [25]. The low STN is a consequence of severe flow localization [37] and is the subject of continuing investigation.

DISCUSSION

The macroscopic changes in mechanical properties such as yield strength and ductility are determined by the microstructure and microcomposition resulting from the irradiation [41,42]. The damage microstructure in austenitic stainless steels irradiated at temperatures up to about 250°C consists of a very high density of small black dot defect clusters, about 2 nm in diameter [4]. The density of these black dots is independent of temperature from 50°C up to about 250°C; at higher irradiation temperatures the black dot density decreases sharply. The density of observable faulted Frank loops, 10 to 20 nm in diameter, increases continuously up to about 300-350°C before decreasing rapidly [4,43,44]. These loops dominate the microstructure at temperatures from about 250 to 400°C. Above irradiation temperatures of about 400°C, the microstructure is dominated by cavities, precipitates, and network dislocations. Small cavities may also be present at temperatures as low as 200°C [45,46].

The changes in yield strength after neutron irradiation can be correlated with the observed changes in microstructure using simple

hardening models [5,42,47-51]. Cavities (both bubbles and voids), Frank loops, black dot defect clusters, network dislocations, and precipitates all contribute to the hardening either as short range or long range obstacles. The qualitative agreement between the models and several sets of data is reasonably good [e.g., 48]. In general, the irradiation defect structure provides a very effective barrier to dislocation motion and raises the yield stress to very high levels. At some critical stress level, dislocations break free, producing a burst of deformation that is sufficient to cause the initial load drop that is seen in Figs. 1-3. This load drop may be due to the onset of a very localized deformation in the form of a Luders-like band associated with dislocation channeling [37]. The subsequent low work hardening rates may also be related to dislocation channeling [42,47,52-56]. Yield stress increases with irradiation temperature until a point is reached where yielding is followed by mechanical instability (Fig. 3). A local reduction in area of the specimen cannot be compensated for by work hardening and deformation concentrates in this region until failure occurs. At 400°C, the barriers to gliding dislocations continue to produce strengthening but, because the spacing of the defects is larger here than in the lower temperature regime, the strengthening is less [4,53,57,58].

The changes in flow properties with irradiation temperature are related to the nature of the defect structure [47]. The dominant microstructural features of each irradiation temperature are superimposed on the dose-temperature map in Fig. 11. In the regime where STN values are less than 1%, the microstructure is dominated by faulted Frank loops and small cavities. Conversely, the STN remains high (greater than 5%) up to at least 40 dpa at temperatures where the microstructure is dominated by black dots (below 200°C) or by large cavities, precipitates and network dislocations (above 400°C). The relationships between the nature and density of radiation defects and deformation and fracture processes are very complex with many unresolved issues [52,59]. For example, the deformation behavior is also dependent on the test temperature and the strain rate [19,24,60]. Additional microscopy and off-temperature tensile tests may help to separate the

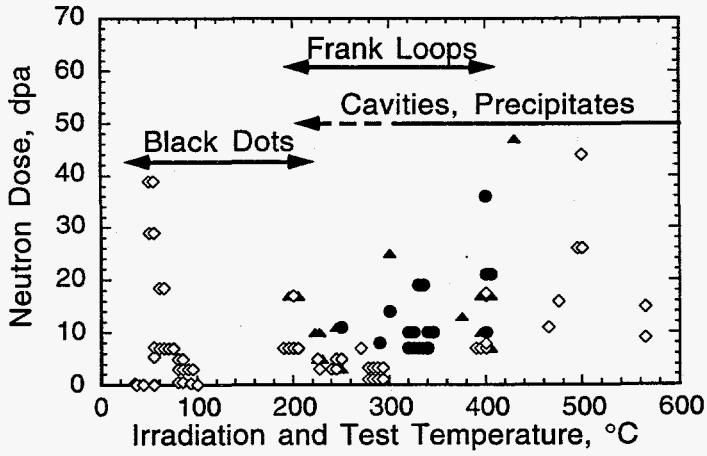

FIG. 11--Dose-temperature map of Fig. 10 with the temperature regions of the dominant microstructural features superimposed.

contributions of the different microstructural features and lead to better modeling techniques.

CONCLUSIONS

A single heat of solution annealed type 316 stainless steel was irradiated to 7 and 18 dpa at 60, 200, 330, and 400°C. The tensile properties as a function of dose and as a function of temperature were investigated. Large changes in yield strength, deformation mode, strain to necking, and strain hardening capacity were seen in this irradiation experiment. The magnitudes of the changes are dependent on both irradiation temperature and neutron dose. Irradiation can more than triple the yield strength over the unirradiated value and decrease the strain to necking to less than 0.5% under certain conditions. A maximum increase in yield strength and a minimum in the STN occur after irradiation at 330°C but the failure mode remains ductile. The macroscopic changes in mechanical properties are determined by the microstructure resulting from irradiation. The radiation-induced defect structure provides effective barriers to dislocation motion and raises yield strength to high levels. In the regime where the yield strength is maximum and STN is minimum, the microstructure is dominated by Frank loops and small cavities. Additional microscopy and off-temperature tensile tests may help to separate the contributions of the different microstructural features and lead to better modeling techniques.

ACKNOWLEDGMENTS

This research was sponsored by the Office of Fusion Energy Sciences, U.S. Department of Energy, under contract DE-AC05-96OR22464 with Lockheed Martin Energy Research Corporation, and the Japan Atomic Energy Research Institute. The tensile testing was performed by R. L. Martin, L. T. Gibson, and W. S. Eatherly. The authors are grateful to Drs. R. L. Klueh and A. N. Gubbi for technical reviews and to Ms. G. L. Burn for preparation of the manuscript.

REFERENCES

[1] M. L. Grossbeck, T. Sawai, S. Jitsukawa, and L. T. Gibson, Fusion Reactor Materials Semiannual Progress Report for Period Ending March 31, 1989, Office of Fusion Energy, DOE/ER-0313/6, 1989, p. 259.

[2] M. L. Grossbeck, Fusion Reactor Materials Semiannual Progress Report for Period Ending March 31, 1989, Office of Fusion Energy, DOE/ER-0313/6, 1989, p. 243.

[3] S. Jitsukawa, P. J. Maziasz, T. Ishiyama, L. T. Gibson, and A. Hishinuma, Journal of Nuclear Materials, Vols. 191-194, 1992, p. 771.

[4] S. J. Zinkle, P. J. Maziasz, and R. E. Stoller, Journal of Nuclear Materials, Vol. 206, 1993, p. 266.

[5] P. J. Maziasz, Journal of Nuclear Materials, Vols. 191-194, 1992, p. 701.

[6] I. I. Siman-Tov, Fusion Reactor Materials Semiannual Progress Report for Period Ending September 30, 1987, Office of Fusion Energy, DOE/ER-0313/3, 1988, p. 7.

[7] L. R. Greenwood, Fusion Reactor Materials Semiannual Progress Report for Period Ending March 31, 1989, Office of Fusion Energy, DOE/ER-0313/6, 1989, p. 23.
[8] L. R. Greenwood and D. V. Steidl, Fusion Reactor Materials Semiannual Progress Report for Period Ending March 31, 1990, Office of Fusion Energy, DOE/ER-0313/8, 1990, p. 34.
[9] L. R. Greenwood, Alloy Development for Irradiation Performance Semiannual Progress Report for Period Ending March 31, 1986, Office of Fusion Energy, DOE/ER-0045/16, 1986, p. 17.
[10] L. R. Greenwood, C. A. Baldwin and B. M. Oliver, Fusion Materials Semiannual Progress Report for Period Ending September 30, 1994, Office of Fusion Energy, DOE/ER-0313/17, 1995, p. 28.
[11] A. W. Longest, J. E. Pawel, D. W. Heatherly, R. G. Sitterson and R. L. Wallace, Fusion Reactor Materials Semiannual Progress Report for Period Ending March 31, 1993, Office of Fusion Energy, DOE/ER-0313/14, 1993, p. 14.
[12] A. W. Longest, D. W. Heatherly, E. D. Clemmer and J. E. Corum, Fusion Reactor Materials Semiannual Progress Report for Period Ending September 30, 1991, Office of Fusion Energy, DOE/ER-0313/11, 1992, p. 17.
[13] A. W. Longest, J. E. Pawel, D. W. Heatherly, R. G. Sitterson and R. L. Wallace, Fusion Reactor Materials Semiannual Progress Report for Period Ending September 30, 1993, Office of Fusion Energy, DOE/ER-0313/15, p. 23.
[14] G. E. Lucas, M. Billone, J. E. Pawel, and M. L. Hamilton, presented at the 7th International Conference on Fusion Reactor Materials, Obninsk, Russia, September 25-29, 1995, and to be published in Journal of Nuclear Materials.
[15] J. E. Pawel, A. F. Rowcliffe, D. J. Alexander, M. L. Grossbeck, and K. Shiba, presented at the 7th International Conference on Fusion Reactor Materials, Obninsk, Russia, September 25-29, 1995, and to be published in Journal of Nuclear Materials.
[16] M. G. Horsten and M. I. de Vries, Effects of Radiation on Materials: 17th International Symposium, ASTM STP 1270, D. S. Gelles, R. K. Nanstad, A. S. Kumar, and E. A. Little, Eds., American Society for Testing and Materials, Philadelphia, 1996, in press.
[17] J. D. Elen and P. Fenici, Journal of Nuclear Materials, Vols. 191-194, 1992, p. 766.
[18] M. G. Horsten and M. I. de Vries, Journal of Nuclear Materials, Vols. 212-215, 1994, p. 514.
[19] M. G. Horsten, J. van Hoepen and M. I. de Vries, Tensile Tests on Plate and Electron-Beam Welded Type 316L(N) Material, Netherlands Energy Research Foundation ECN, ECN-CX--93-112, 1993.
[20] M. I. de Vries, Private Communication.
[21] A. A. Tavassoli, Assessment of Austenitic Stainless Steels, ITER Task BL-URD3, N.T. SRMA 94-2061, Revision June 1994.
[22] R. Kallstrom, B. Josefsson and Y. Haag, Results From Tensile Testing of 316L Plate and Weld Material, Studsvik Material AB, Sweden, STUDSVIK/M-93/45, PSM 1-1, 1993.
[23] H. L. Heinisch, Journal of Nuclear Materials, Vols. 155-157, 1988, p. 121.
[24] J. E. Pawel, M. L. Grossbeck, A. F. Rowcliffe and K. Shiba, Fusion Materials Semiannual Progress Report for Period Ending September 30, 1994, Office of Fusion Energy, DOE/ER-0313/17, 1994, p. 125.

[25] B. Van der Schaaf, M. Grossbeck, and H. Scheurer, Oak Ridge Test Matrix No. 5B and 5C HFR and HFIR Irradiations and Post-Irradiation Tensile Tests in Support of Fusion Reactor First Wall Material Development, Nuclear Science and Technology, Commission of the European Communities, Luxembourg, EUR 10659 EN, 1986.
[26] F. W. Wiffen and P. J. Maziasz, Journal of Nuclear Materials, Vols. 103&104, 1981, p. 821.
[27] H. R. Higgy and F. H. Hammad, Journal of Nuclear Materials, Vol. 55, 1975, p. 177.
[28] E. E. Bloom, W. R. Martin, J. O. Stiegler, and J. R. Weir, Journal of Nuclear Materials, Vol. 22, 1967, p. 68.
[29] W. R. Martin and J. R. Weir, in Flow and Fracture of Metals and Alloys in Nuclear Environments, ASTM STP 380, American Society for Testing and Materials, Philadelphia, 1965, p. 251.
[30] H. L. Heinisch, M. L. Hamilton, W. F. Sommer, and P. D. Ferguson, Journal of Nuclear Materials, Vols. 191-194, 1992, p. 1177.
[31] R. L. Klueh, Alloy Development for Irradiation Performance Semiannual Progress Report for Period Ending March 31, 1984, Office of Fusion Energy, DOE/ER-0045/12, 1984, p. 45.
[32] M. J. Makin, in Radiation Effects, Metallurgical Society Conferences, Vol. 37, W. F. Sheely, Ed., Gordon and Breach, Science Publishers, Inc., New York, 1967, p. 629.
[33] M. L. Grossbeck, Journal of Nuclear Materials, Vols. 179-181, 1991, p. 568.
[34] G. R. Odette and G. E. Lucas, Journal of Nuclear Materials, Vols. 179-181, 1991, p. 572.
[35] M. L. Grossbeck, K. Ehrlich, and C. Wassilew, Journal of Nuclear Materials, Vol. 174, 1990, p. 264.
[36] A. J. Jacobs, G. P. Wozadlo, K. Nakata, T. Yoshida, and I. Masaoka, Environmental Degradation of Materials in Nuclear Power Systems--Water Reactors, G. J. Theus and J. R. Weeks, Eds., The Metallurgical Society, Inc., Warrendale, PA, 1988, p. 673.
[37] J. E. Pawel, A. F. Rowcliffe, G. E. Lucas, and S. J. Zinkle, presented at the 117th Meeting of the Japan Institute of Metals: International Symposia on Advanced Materials and Technology for the 21st Century, Honolulu, Hawaii, December 12-15, 1995, and to be published in Journal of Nuclear Materials.
[38] S. Majumdar, Fusion Engineering and Design 29, 1994, p. 158.
[39] M. L. Grossbeck and P. J. Maziasz, Journal of Nuclear Materials, Vols. 85&86, 1979, p. 883.
[40] K. Shiba, S. Jitsukawa, J. E. Pawel and A. F. Rowcliffe, Fusion Reactor Materials Semiannual Progress Report for Period Ending September 30, 1993, Office of Fusion Energy, DOE/ER-0313/15, 1994, p. 181.
[41] L. K. Mansur, Kinetics of Nonhomogeneous Processes, G. R. Freeman, Ed., John Wiley & Sons, Inc., New York, 1987 p. 377.
[42] G. E. Lucas, Journal of Nuclear Materials, Vol. 206, 1993, p. 287.
[43] P. J. Maziasz, Journal of Nuclear Materials, Vol. 205, 1993, p. 118.
[44] P. J. Maziasz and D. N. Braski, Journal of Nuclear Materials, Vols. 122 & 123, 1984, p. 311.
[45] S. J. Zinkle and R. L. Sindelar, Journal of Nuclear Materials, 155-157, 1988, p. 1196.
[46] S. J. Zinkle, private communication, 1996.

[47] G. R. Odette and D. Frey, Journal of Nuclear Materials, Vols. 85 & 86, 1979, p. 817.
[48] M. L. Grossbeck, P. J. Maziasz and A. F. Rowcliffe, Journal of Nuclear Materials, Vols. 191-194, 1992, p. 808.
[49] H. R. Brager, L. D. Blackburn and D. L. Greenslade, Journal of Nuclear Materials, Vols. 122 & 123, 1984, p. 332.
[50] F. A. Garner, M. L. Hamilton, N. F. Panayotou, and G. D. Johnson, Journal of Nuclear Materials, Vols. 103 & 104, 1981, p. 803.
[51] R. L. Simons and L. A. Hulbert, Effects of Radiation on Materials: 12th International Symposium, ASTM STP 870, F. A. Garner and J. S. Perrin, Eds., American Society for Testing and Materials, Philadelphia, 1985, p. 820.
[52] M. S. Wechsler, The Inhomogeneity of Plastic Deformation, R. E. Reed-Hill, Ed., American Society for Metals, Metals Park, Ohio, 1973, p. 19.
[53] M. L. Grossbeck, J. O. Stiegler and J. J. Holmes, Radiation Effects in Breeder Reactor Structural Materials, M. L. Bleiberg and J. W. Bennett, Eds., The Metallurgical Society of AIME, New York, 1977, p. 95.
[54] L. K. Mansur and M. L. Grossbeck, Journal of Nuclear Materials, Vols. 155-157, 1988, p. 130.
[55] R. L. Fish, J. L. Straalsund, C. W. Hunter and J. J. Holmes, Effects of Radiation on Substructure and Mechanical Properties of Metals and Alloys, ASTM STP 529, J. Moteff, Ed., American Society for Testing and Materials, Philadelphia, 1973, p. 149.
[56] M. S. Wechsler, Fundamental Aspects of Radiation Damage in Metals, M. T Robinson and F. W. Young, Jr., Eds., U. S. Energy Research and Development Administration, CONF-751006, Gatlinburg, Tennessee, 1975, p. 991.
[57] E. E. Bloom, Radiation Damage in Metals, N. L. Peterson and S. D. Harkness, Eds., American Society of Metals, Metals Park, OH, 1976, p. 295.
[58] D. R. Harries, Journal of Nuclear Materials, Vols. 82, 1979, p. 2.
[59] R. D. Carter, M. Atzmon, G. S. Was, and S. M. Bruemmer, Microstructure of Irradiated Materials, Materials Research Society Symposium Proceedings, Vol. 373, I. M. Robertson, L. E. Rehn, S. J. Zinkle, and W. J. Phythian, Eds., Materials Research Society, Pittsburgh, 1995, p. 171.
[60] J. L. Brimhall, J. I. Cole, J. S. Vetrano, and S. M. Bruemmer, Microstructure of Irradiated Materials, Materials Research Society Symposium Proceedings, Vol. 373, I. M. Robertson, L. E. Rehn, S. J. Zinkle, and W. J. Phythian, Eds., Materials Research Society, Pittsburgh, 1995, p. 177.